

Scalable Production of Nanofiber Filtration Membranes via Solution Blow Spinning

Jeremy Baum, Danielle Fansi, Brian Heligman, Louis Levine, Zachary Pelczar, Oliver Zhao

Abstract

As of 2016, almost four billion people in the world do not have access to clean water ^[1]. One common technique for water purification is microfiltration, where the micron sized pores exclude larger pathogenic contaminants. A cheap, scalable technique for the production of these filters could allow for greater access to clean drinking water globally. Nanofiber mats have shown exceptional performance in the microfiltration regime, but current production techniques have had difficulty scaling to industrial levels. The solution blow spinning technique offers a promising avenue for large-scale production of these nanofiber microfilters. In this report, we design a filter composed of a nanofiber mat deposited upon a mechanically durable scaffold structure. We then analyze the strength and filtration properties of our mats, and compare it to commercially available products. We then produce a preliminary prototype of a blow spun nanofiber filter, and characterize these mats to further enhance our understanding of the behavior of the non-woven fiber structure. Finally, we present future directions of our research, including computational fluid dynamic modeling, optimization of deposition procedures, and more comprehensive testing of the filters.

Motivation

In 2016, it was estimated that approximately 4 billion people worldwide lack access to safe drinking water, resulting in 9.7% of all worldwide deaths under the age of five^[1]. In recent years, there has been significant interest in the use of polymer nanofiber mats as filtering membranes due to their high specific surface area and their ease of functionalization ^[2]. Materials such as polypropylene (PP), polyvinylidene fluoride (PVDF), cellulosic derivatives (CD), polyacrylonitrile (PAN)^[3] and other polymers have all been successfully commercialized as microfiltration membranes. While nanofiber membranes have been shown to display exceptional performance, the traditional production technique of electrospinning suffers from slow deposition rates^[4], which increases costs and makes industrial scaling more difficult. In recent work, Medeiros et al. discovered an alternative deposition technique called solution blow spinning ^[3]. Blow spinning is an analog of electrospinning that allows for the rapid deposition of polymer nanofibers on a broad range of substrates, overcoming many of the limitations plaguing electrospinning ^{[4][5]}. In this work, we investigate potential production of microfiltration membranes using this technique.

Previous Work

The majority of work surrounding the production of polymer nanofibers has focused on the electrospinning method. In electrospinning, a polymer solution is pulled from a thin orifice by a voltage differential, and as the solvent evaporates from the system, polymer nanofibers are formed. The morphology of the nanofibers can be controlled by varying the thickness of the needle, the applied current, and the physical properties of the liquid polymer feed (i.e. flow rate, viscosity, and conductivity) [5]. However, production of polymer nanofibers by electrospinning is hindered by two major issues: scalability and polymer solution restrictions. The production scaling options are limited; typical needle/charged plate method deposition rates are incredibly slow (on the order to 10g/hour). Possible solutions to these limitations are available through products like El Marco's NanoSpider or Revolution Fiber's "Sonic Electrospinning Technology" which process polymer solutions in sheets, instead of by a droplet in a needle, making roll-to-roll processing possible. This results in deposition rates of up to 60m/min (1.6m wide rolls) for the Nanospider, or 500m² for Revolution Fiber's system. However, the complexity of these systems have prevented their wide-scale adoption. In short, the limited scalability of electrospinning continues to be an issue in generating large quantities of nanofiber mats.

Solution blow spinning is a potentially more affordable and scalable when compared to electrospinning, without requiring costly equipment. In this technique, the polymer solution is pulled from an orifice by a pressure gradient instead of a voltage differential. While the process of blow spinning is limited to the same material precursors as electrospinning, it has been shown to create polymer fibers at a much more rapid rate. Blow spinning has been shown to provide similar quality fiber networks with very little of the equipment required for electrospinning [4]. The ability to rapidly deposit on any substrate makes blow spinning an attractive choice for low cost and high scalability manufacturing.

Design Goals

The goal of this project was to design a low cost filtration system that could help reduce the risk of drinking unclean water. Microfiltration was deemed the most appropriate technique to accomplish this goal due its ability to remove many of the risk factors in unclean water, specifically bacteria without a significant energy cost. Throughout the design process, a continued focus was placed on minimizing system cost and environmental impact while maintaining high performance. Although microfiltration does not completely sterilize dirty water, it is our hope that the designed filter will improve the quality of life for those who have limited access to existing filtration systems.

The design of our filter had six major steps which are outlined in Figure 1. We began the design process by introducing details of microfiltration and stating what particles can be filtered by this technique. Then, we decided upon what material we are using to fabricate our filter based on analysis of cost and other material properties. Next, we chose a specific processing technique to produce our filter. Afterwards, we conducted preliminary prototyping to determine properties of our filter as well as computational modeling; both of which fed into the preliminary modeling of our filter. Based on the

results of the preliminary mathematical modeling, we added a scaffold to the filter setup to maximize the flow rate of our filter for a given pressure.

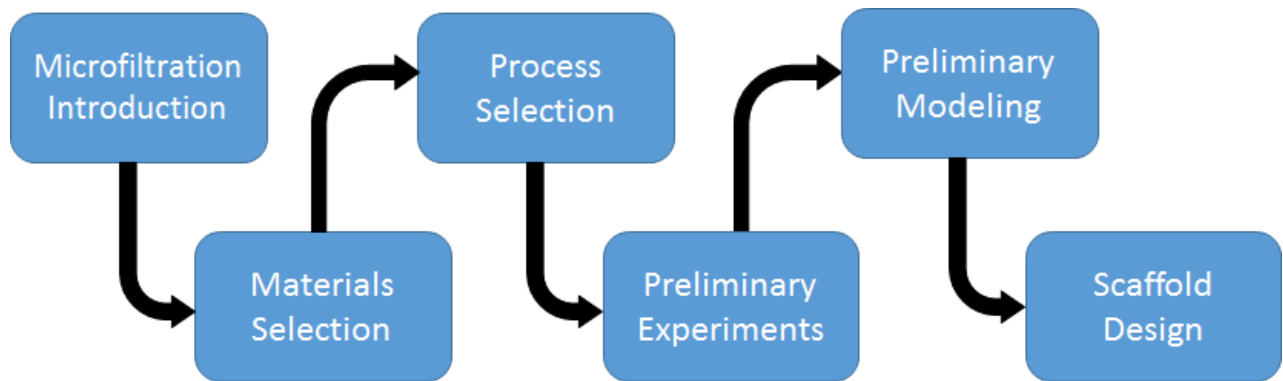


Figure 1. Flowchart of the filter design process.

Technical Approach

1. An Introduction to Microfiltration

Pressure driven membrane filtration is one of the most energy efficient forms of water purification [7]. These techniques are typically classified by the pore size of the filter membrane, and include microfiltration (0.1-10 μm), ultrafiltration (2-100 nm), and nanofiltration (<1 nm). Microfiltration can be used to remove particulates from a liquid including yeast, sand, E-coli, fecal coliform, red blood cells, bacteria, and protozoa [8]. Bacterial and protozoan infections are responsible for a significant portion of the 1-2 million diarrheal deaths each year [9], and their removal is particularly important. Although microfiltration is unable to remove viruses and other nanoscale disease vectors from water, it has a significantly reduced energy cost compared to other techniques [10]. This is because any reduction in pore size increases the minimum pressure to force liquid through a membrane. Microfiltration is typically operated between 100-400 kPa, while nanofiltration requires 600-1000 kPa. The upper limit on operating pressure is a result of diminishing efficiency due to the formation of an undesirable particulate buildup above the membrane. The lower limit is the pressure necessary to move water through microfiltration pore sizes. Although microfiltration does not completely sterilize water, it provides an immediate low-cost improvement in water quality, and simplifies further sterilization procedures.

2. Materials Selection

Both polymers and ceramics can be used for the production of microfiltration membranes. Ceramics have high chemical compatibility, excellent thermal stability and long operational life, but are limited by their lower permeability and higher cost [11]. Polymeric membranes are more flexible and inexpensive, but traditional solvent casting approaches have produced membranes with an asymmetric

structure resulting in low surface porosity [7]. We decided to focus on polymeric materials, as we found their lower material and processing costs extremely attractive.

We narrowed the field of potential materials for our membranes to polyvinylidene fluoride (PVDF) [5], poly-lactic acid (PLA) [6], and cellulose acetate (CA) based on their low cost, mechanical strength, and chemical stability. To compare our materials of interest, a selection graph (Figure 2) was created using CES EduPack, taking into consideration the mechanical strength and cost of each material. Strength is important because the membrane must be able to withstand the forces resultant from the applied pressure gradient. Cost remains an important aspect in our material selection as well; one of our main goals is to create a cheap and scalable membrane. PVDF was initially considered a strong option, due to its extensive applications in mechanically strong polymer coatings and commercial filters. However, it is both costly and non-environmentally friendly. Cellulose acetate (CA) has good mechanical strength, environmentally friendliness, and is relatively cheap. Of all the candidate materials, PLA has the highest mechanical strength, while remaining less expensive than both PVDF and CA. PLA is also highly processable, and completely biodegradable. Although PLA has not been explored extensively as a membrane material, it is an attractive option for potential filter applications and was selected for this project.

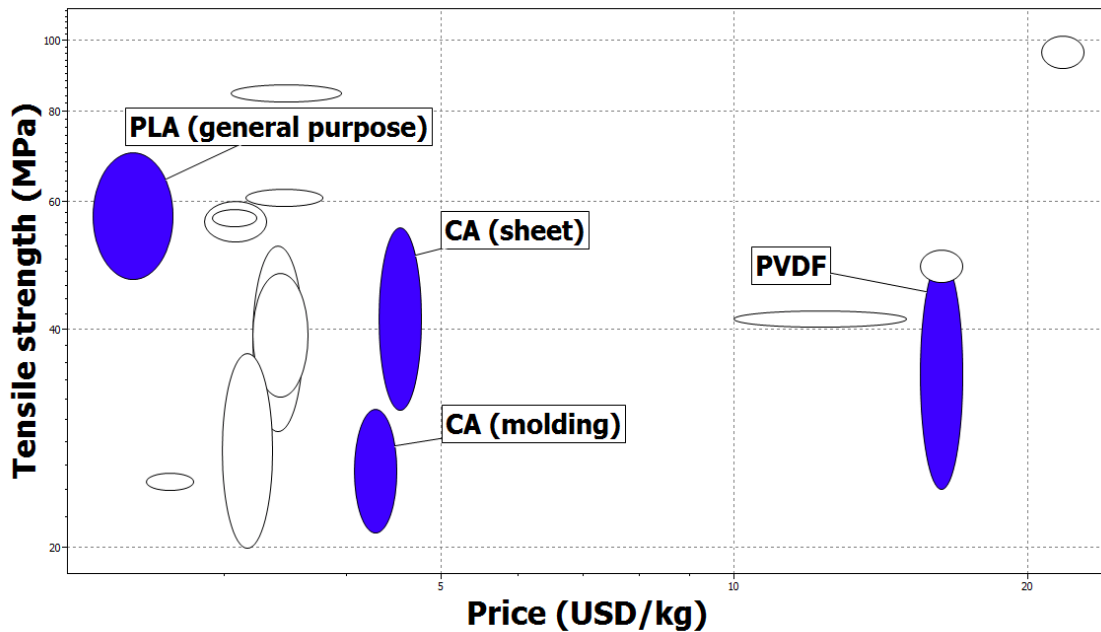


Figure 2. Tensile strength vs. Price graph comparing material selection options.

3. Process Selection

After selection of the membrane material, we needed to choose a processing technique for fabricating the filters. There are multiple methods for the creation of micron-pore sized membranes, but each technique has limitations. Solution casting, or the formation of films through the evaporation of a solvent-polymer mixture, is an extremely common technique for the processing of polymers. However,

the processing of films in this manner typically has resulted in an asymmetric structure with low surface porosity^[7]. Membranes composed of nonwoven nanofibers offer improved performance when compared to conventional polymer membranes, due to higher porosity and a unique continuously interconnected pore structure^[7]. These mats are commonly produced via electrospinning, a technique which produces high quality, non-woven fiber mats. In this method, a polymer solution is fed through a charged needle. At sufficient voltages, the electrostatic forces attracting the droplet to a charged substrate counteract the surface tension of the liquid, forming a thin strand of liquid known as a “Taylor cone” (Figure 3). As the Taylor cone is stretched towards the substrate, the solvent evaporates, forming a nanoscale polymer strand. However, electrospinning is time consuming, expensive, and suffers from extremely low deposition rates. In solution blow spinning, a pressure gradient, rather than a voltage differential, is used to produce a Taylor cone. As high pressure gas flows around the needle of an airbrush, polymer solution is fed into the device, and a Taylor cone forms at the end of the needle. Again, the solvent evaporates, and nanoscale fibers are formed. Solution blow spinning does not require the extensive set-up or high voltage of the electrospinning apparatus, and deposits polymers at a more rapid rate^[4]. The low capital required for laboratory experimentation with blow spinning allows for rapid prototyping of small scale batches of fibers, while also allowing for eventual scaling to roll to roll techniques. We believe that these beneficial characteristics of blow spinning outweigh the ability of electrospinning to better control fiber alignment^[12]. For these reasons, we chose to use pursue blow spinning as the processing method for our nanofiber membranes.

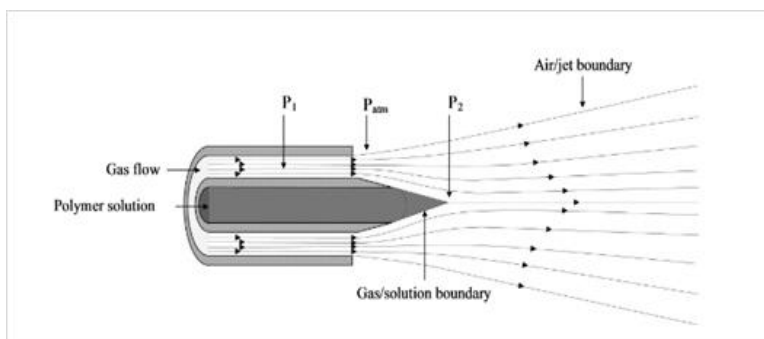


Figure 3. A Taylor cone will form at the end of the needle of an airbrush, where a thin strand of polymer solution is ejected and solidifies on its way to the target, producing nano-sized fibers.^[4]

Filters with 0.2 μm pores have been commonly studied due to their prevalence in industry, and research has shown them to be capable of completely excluding bacterial pathogens^[13]. In order for our filter to have the desired antibacterial properties, our nanofiber mat must have at least this 0.2 μm pore size. To ensure we reach this desired pore size, it is important to develop a relationship between the blow spinning deposition parameters and membrane pore size.

In a study by Wang et al. nonwoven PAN fiber mats were generated with a variety of fiber diameters between 100 and 1000 nanometers^[7]. These mats were then characterized by pore size, and a linear trend was found between pore size and fiber diameter. As shown in Figure 4, as fiber diameter

was decreased, pore size also decreased. In addition, a fiber diameter of 100-150 nanometers was shown to produce pore sizes of approximately 0.2 μm .

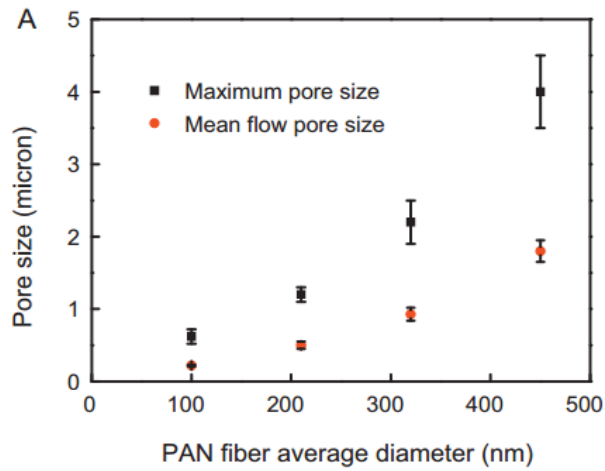


Figure 4. Relationship between fiber diameter and pore size ^[7]

A computational model to replicate nanofiber mats produced by solution blow spinning was created with the ANSYS Mechanical package in conjunction with the ANSYS Parametric Design Language (APDL). This model, made possible by the thesis of Rahul Vallabh of North Carolina State University, allows us to characterize the physical properties of a mat, such as porosity or pore area, based on an input fiber diameter, as well as perform computational dynamics on the model.

Using ANSYS, we confirmed the established relationship between fiber diameter and pore size using computer generated fiber mats with fiber diameters between 50nm and 900nm. First, fibers of a chosen diameter were randomly generated in discrete layers. Then, a pore volume which encompasses the fibers was created, followed by a subtraction of the fibers from this pore network. This generated a model of the pore volume, which is useful for fluid dynamics, where a negative model is necessary (Figure 5B), though a model of only fibers can be generated as well (Figure 5).

These models can be imported into a design program, such as Solidworks, and porosity can be determined through built in object volume calculations. The results are displayed in Table 1. This data, along with the experimental data obtained by Wang et al. clearly establishes the relationship between fiber diameter and membrane pore size.

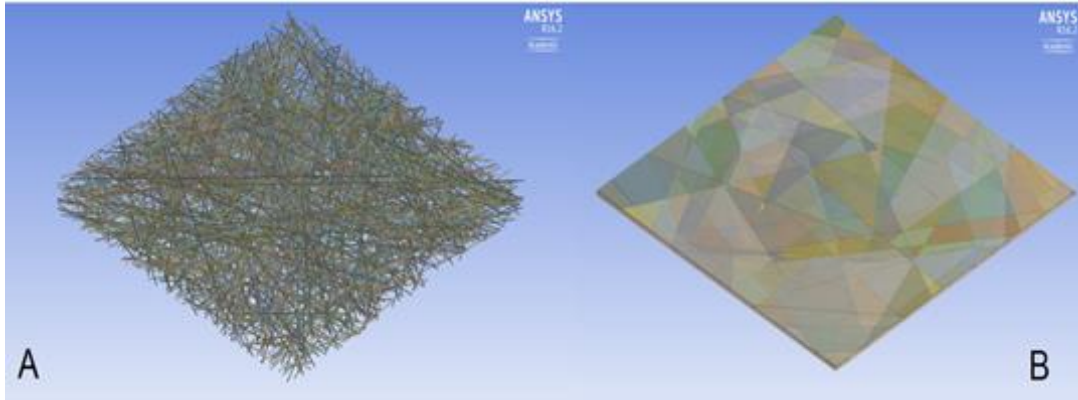


Figure 5. a) Randomly generated fiber mat b) Randomly generated pore volumes, which is the inverse of the fiber mat. The pore volumes more useful for modeling the CFD because the inverse geometry is easier to input into the Fluent software.

Table 1. Relationship between fiber thickness, porosity, and average pore size.

Fiber thickness	50 nm	150 nm	300 nm	900nm
Porosity	99.07 %	97.48%	94.82%	86.77%
Average Pore Size (Diameter)	1.09 μm	1.18 μm	1.34 μm	3.06 μm

For the solution blow spinning method, polymer solution concentration has been shown to have the single most profound effect on fiber morphology of any blow spinning parameter ^[14]. Low viscosities, and thus low polymer concentration, correlates to smaller fiber diameters. This dependence is related to the higher mobility of polymer chains in the blow spun jet during the deposition process. A secondary controlling parameter, flow rate, is also shown to have a non-negligible effect on fiber diameter. Oliveira et al. show that an increase in flow rate correlates to a decrease in fiber diameter due to an increased solvent evaporation rate ^[14]. In order to achieve fiber mats that meet our requirement of 0.2 μm pore diameter, we have chosen to use a relatively low polymer solution concentration of 5 wt%, and a high flow rate for our initial fiber mat deposition.

4. Preliminary Experimentation for Material Properties

In our initial calculations, we used literature values for tensile strength and stiffness of PLA [15]. However, these values were taken from bulk materials, and we felt it necessary to take our own measurements in order to correct these values if necessary. Thus, we created a set of PLA blow spun nanofiber mats using a commercially available airbrush, and a 5 weight percent PLA in THF precursor. 15 cubic feet per hour CO₂ was used to generate the pressure differential. These mats were characterized in a Hitachi S-4500 Scanning Electron Microscope, where we could determine fiber diameter and mat thickness (Figure 6). In order to prevent charging of the polymer fibers, the mats were briefly sputter coated (<1 sec deposition) with carbon, enough to make the sample conductive, but not enough to significantly affect morphology. The images show that our fiber diameters ranged from 0.20 μm to 0.37 μm which is close to our target goal of 100 – 200 nm fiber diameter. With fiber diameters in this target 100 – 200nm range, we would theoretically have pore sizes of around 0.2 μm based on data from literature.

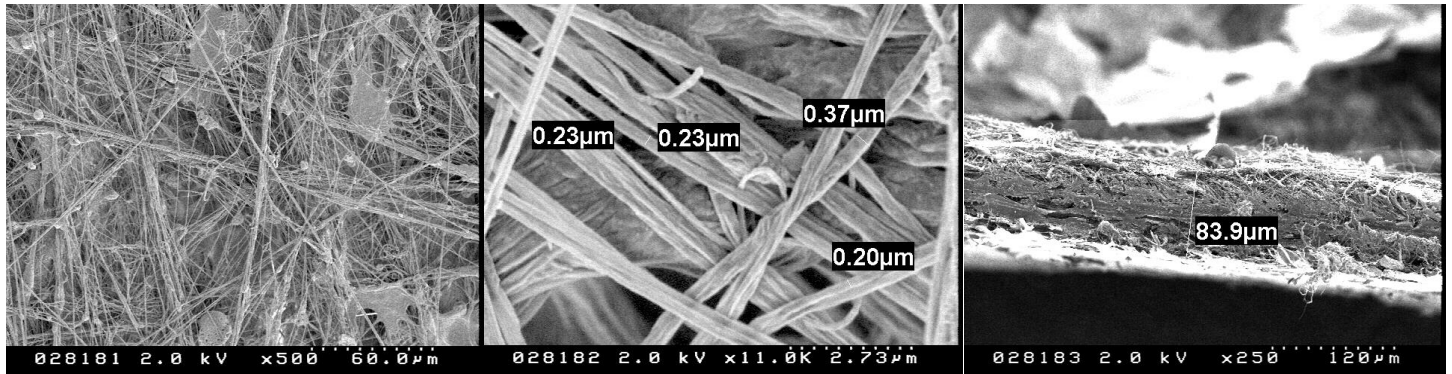


Figure 6. SEM images of blow spun PLA nanofiber

Fiber mats created under the same conditions as those studied in the SEM were taken to the Functional Macromolecular Laboratory in the Kim Building, where they were tested on a Dynamic Mechanical Analyzer (DMA). In order to make mats substantial enough for testing, we used a long deposition time and large area to produce samples of 0.5cm x 2cm x 700 μm dimensions, with fiber diameter between 100nm and 300nm. Through DMA testing, our polymer mats were determined to have a Young's modulus of 20.8 MPa and a yield strength of 850 kPa.

5. Preliminary Mathematical Modeling

We have two mathematical models to determine the design parameters for a filter membrane. The first model is used to relate the pure water permeability, L_p , to the membrane thickness, also referred to as pore depth. Pure water permeability is defined as the volume of water that passes through a membrane per unit time, per unit area and per unit of operating pressure. The second model relates the

burst pressure, Δp , to the pore depth and other mechanical properties of the membrane. Burst pressure is defined to be the pressure at which the membrane will break.

Water Permeability Model

Equation 1 shows the Hagen-Poiseuille equation which describes the exact relationship between pure water permeability and pore depth. Here μ is the dynamic viscosity of water, A_k is the surface porosity of the membrane, r_p is the radius of the pore, and ΔX is the pore depth. This pore diffusion model assumes that the pores have a cylindrical shape and are completely straight. Because the structure of electrospun fiber mats is very porous, the pores in the membrane have low tortuosity, meaning they are almost completely straight. As a result, the approximation taken by the Hagen-Poiseuille equation is accurate for our membrane filter design ^[16].

$$L_p = \frac{r_p^2 A_k}{8\mu\Delta X} \quad [1]$$

Assuming the water is being filtered is at 25°C, the dynamic viscosity of water, μ has a value of 8.9×10^{-4} Pa*s at 25°C ^[17]. The radius of the pore, r_p was set to be 0.1 μ m in order to satisfy microfiltration conditions. The surface porosity was set to be 0.85, based on values found from literature of an electrospun polyacrylonitrile/non-woven polyethylene terephthalate composite nanofiber membrane ^[7].

Burst Pressure Model

Equation 2 shows the exact relationship between burst pressure and pore depth ^[23]. Here ν is the Poisson's ratio, E is the Young's modulus, σ_y is the yield stress, σ_0 is the residual stress, r_M is the radius of the membrane, and ΔX again is the pore depth.

$$\Delta p = 4\left(\frac{\Delta X}{r_M}\right)\sigma_y \sqrt{1.5 * (\sigma_0 - \sigma_y) \frac{1-\nu}{E}} \quad [2]$$

For our calculations, we chose to use a membrane radius, r_M of 45 mm, as it is the size of commercially available membrane filters ^[3]. The Young's modulus and yield stress are both determined from the DMA test explained in the previous section, with values of 20.8 MPa and 850 kPa respectively. The Poisson's ratio value of 0.3 was determined based on the tested value of an electrospun PVDF membrane ^[18]. Although the process and material used for the value of Poisson's ratio are different than our membrane, the value obtained from literature is still of a nanofiber membrane, and can be used as a reasonable estimate of the material property. The residual stress, σ_0 , was determined to be 56.3 MPa by taking experimental values of burst pressure, Young's modulus, yield stress, and Poisson's ratio of a PLA nanofiber membrane and solving for residual stress using Equation 2 ^[15].

Determining a Membrane Thickness

In order to create a filter which can safely operate without failure, we need to design a membrane which has a burst pressure larger than the operating pressure. As a result, we chose to define the operating pressure to be 4/5 as large as the burst pressure to account for this safety factor. Equation 2 is now modified to become Equation 3 where p represents the operating pressure of the filter.

$$p = 1.25 * \Delta p = 4 \left(\frac{\Delta X}{r_M} \right) \sigma_y \sqrt{1.5 * (\sigma_0 - \sigma_y) \frac{1-\nu}{E}} \quad [3]$$

We establish that the operating pressure must be 400 kPa, as it is highest pressure in the operating pressure range of 100-400 kPa for microfiltration. Based on this burst pressure constraint, we can calculate our membrane's thickness.

$$1.25 * 400 \text{ kPa} = 4 \left(\frac{\Delta X}{45 \text{ mm}} \right) 0.85 \text{ MPa} \sqrt{1.5 * (56.3 \text{ MPa} - 0.85 \text{ MPa}) \frac{1-0.3}{20.8 \text{ MPa}}} \quad [4]$$

$$\Delta X = 3.96 \text{ mm} \quad [5]$$

The thickness shown in Equation 4 is the minimum thickness that the filter must be in order for the filter to operate at 400 kPa. Now, substituting this value into Equation 1, we can determine the water permeability of our membrane.

$$L_p = \frac{(0.1 * 10^{-6} \text{ m})^2 (0.85)}{8(8.9 * 10^{-4} \text{ Pa} * \text{s})(8.79 * 10^{-3} \text{ m})} = 1.36 * 10^{-10} \frac{\text{m}}{\text{Pa} * \text{s}} \quad [6]$$

Existing commercial filters with a pore radius of 0.11 μm have a water permeability of $2.5 * 10^{-9} \text{ m}/(\text{s} * \text{Pa})$ [19]. When comparing our membrane's water permeability to existing commercial water filters, our membrane's water permeability is almost one order of magnitude lower. This result is unsurprising given the large value we calculated for the thickness of the membrane. While our filter must be nearly 4mm thick to withstand the described pressure gradient, the commercial filter is a mere 100 μm . This is because the relatively low strength of our non-woven fiber mats forces us to compensate by increasing membrane thickness, and decreasing water permeability.

6. Scaffold Design

We then began considering ways that we could strengthen our nanofiber mats. Initially, we had considered annealing of the membrane, but that was shown to change both the pore size and porosity of the membrane. However, we realized that one of the strengths of solution blow spinning is its ability to deposit on any substrate. We decided we would deposit our fibers on a porous, mechanically durable support structure, and began design of this scaffold. This set-up is shown in Figure 7 below.

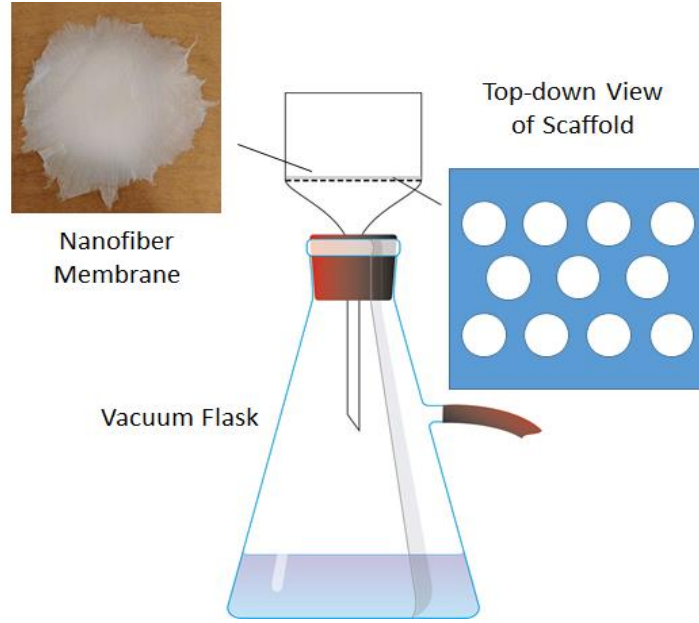


Figure 7. Schematic of our prototyping setup with the filter resting on top of a scaffold with circular holes.

The purpose of the scaffold is to mitigate the pressure that the membrane undergoes during the filtration process. By restricting the regions of the filter through which water can flow, and providing support to the thin membrane, we can increase the pressure at which the membrane will fail. This is shown to be true by the inverse relationship between the radius of the membrane and the burst pressure in Equation 2. If we substitute the radius of the membrane, r_M , with the radius of each individual hole in the scaffold r_H , Equation 2 then becomes Equation 7.

$$\Delta p = 4 \left(\frac{\Delta X}{r_H} \right) \sigma_y \sqrt{1.5 * (\sigma_0 - \sigma_y) \frac{1-\nu}{E}} \quad [7]$$

Effect of Scaffold on Water Permeability

For our modeling, we chose the shape of the scaffold to be a square with closely packed circular holes. In order to determine the optimal size of the holes of the scaffold, it becomes important to examine the dependence of porosity on the hole size. Based upon the limits of injection molding, it was determined that a 0.5mm border would be required between any two holes^[20]. This limitation, combined with a public database of closely packed circles was used to determine scaffold porosity^[21].

The effect of the scaffold on water permeability can be accounted for by multiplying Equation 1 with a scaling factor equivalent to the porosity of the scaffold. The modified equation then becomes Equation 8, where A_m represents the porosity of the scaffold.

$$L_p = \frac{r_p^2 A_k A_m}{8\mu\Delta X} \quad [8]$$

Determining the Scaffold Hole Radius

The metric which we need to optimize in order to create the best filter is *flux*, j . Water permeability, which is in units of $m/(s*Pa)$, can be converted to flux by multiplying by the operating pressure of the membrane. By multiplying Equations 7 and 8, we can obtain the flow rate of our filter.

$$j = L_p * \Delta p = \frac{r_p^2 A_k A_m}{8\mu\Delta X} 4 \left(\frac{\Delta X}{r_H}\right) \sigma_y \sqrt{1.5 * (\sigma_0 - \sigma_y) \frac{1-\nu}{E}} \quad [9]$$

Equation 9 illustrates that flux, j , is independent of thickness for constant pressure conditions. It is instead dependent on the ratio of scaffold porosity/hole size, A_m/r_H , when each of the other variables in Equation 9 are held constant. Equation 10 shows that if we maximize this ratio, we can then maximize the flow rate and consequently the performance of our filter.

$$j = L_p * \Delta p \propto \frac{A_m(r_H)}{r_h} \quad [10]$$

The problem of densely packing circles within a square has already been solved. With the constraint of 0.5 mm between each hole in the scaffold, we can plot the dependence of A_m/r_H , on hole radius as shown in Figure 8. From Figure 8, we can see that the values which corresponds to a maximum of A_m/r_H , are a **0.225 mm** radius and a **0.191** scaffold porosity.

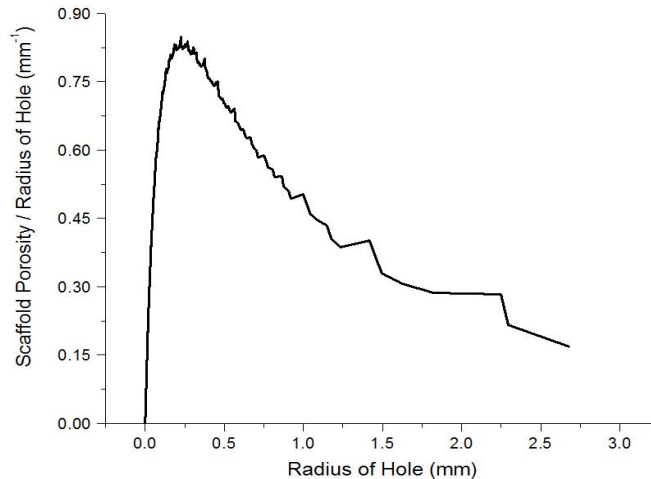


Figure 8. Plot of the dependence of Scaffold Porosity/Radius of Hole on the Radius of the Hole

Redesigning the Membrane Thickness

Again, if we choose the operating pressure to be 400 kPa and the burst pressure to be a factor of 1.25 as large, we can solve for the minimum thickness of the membrane.

$$1.25 * 400kPa = 4\left(\frac{\Delta X}{0.225mm}\right)0.85MPa \sqrt{1.5 * (56.3MPa - 0.85MPa) \frac{1-0.3}{20.8MPa}} \quad [11]$$

$$\Delta X = 1.98 * 10^{-5} m \quad [12]$$

We can now calculate the water permeability with our new membrane thickness, which is shown in Equation 12.

$$L_p = \frac{r_p^2 A_k A_m}{8\mu\Delta X} = \frac{(0.1*10^{-6}m)^2 (0.85)(0.191)}{8(8.9*10^{-4}Pa*s)(1.198*10^{-5}m)} = 1.90 * 10^{-8} \frac{m}{Pa*s} \quad [13]$$

When we again compare this value to literature, we can see that our water permeability is now almost one order of magnitude larger than the permeability of commercial filters, which is $2.5*10^{-9} m/(s*Pa)$ [19]. This is likely due to the high porosity of our nanofiber filters. The addition of the scaffold allows us to continue operating at the upper limit of the microfiltration pressure regime with a competitive water permeability.

Materials Science and Engineering Aspects

This project addressed each component of the structure, properties, and processing interrelationship that defines materials science and engineering. We specifically examined the relationship between the microstructure, pore size, and the porosity of the fiber mat, as well as their dependence on processing parameters. We characterized the mechanical durability of the nonwoven fabric membrane, and use those measurements to calculate the expected burst pressure. We also examined the performance of our nanofiber mat using turbidity testing. Finally, we analyze the processing technique of blow spinning in order to understand how our experimental conditions affect the fiber morphology.

Intellectual Merit

Nanofibers as materials have interesting properties due to their low dimensionality and high surface area to volume ratio. There has been significant interest in the deposition of polymer nanofibers into nonwoven mats due to their excellent mechanical properties and ease of functionalization. A significant amount of research has gone into the development of the electrospinning technique for

polymer fiber deposition, now an extremely mature field with applications across a broad range of disciplines. However, much less is known about solution blow spinning. No comprehensive studies on the design and morphology of a blow spun membrane have been published, and a deeper fundamental understanding of the process is required for the true potential of the technique to be understood. Through characterization methods such as SEM and DMA, we have gained an understanding into the properties of solution blow spun membranes as microfilters.

Ethics and Environmental Impact

The main ethical impact of this project was the possibility of a cheaper alternative for microfilters, providing the opportunity for more clean water. The implementation of blow spinning has the potential to reduce production costs and increase scalability, thereby increasing the accessibility of clean water worldwide. There will likely be no other significant ethical problems with research into this topic.

Our material choice has a low environmental impact. PLA is plant based instead of petroleum based, and is fully biodegradable with a 3-6 month degradation time^[15]. In addition, PLA is fully recyclable; used filters can be cleaned, re-dissolved in solvent, purified and respun. Additionally, blow spun polymer fiber mats do not generate large amounts of waste by energy or byproducts. To provide detailed information to potential users of the end product and reduce product failure, assurance testing will be done to guarantee reliability and quality. Both computer modeling and product testing will be done to ensure a reproducible and effective final product without physical waste.

Broader Impacts

The end goal for this project was to identify a method for the production of nanofiber membranes which is affordable and accessible, while being scalable to a roll-to-roll manufacturing level. The fabrication of nanofiber membranes via solution blow spinning provides high productivity, low-operational cost, and is 100 times faster than electrospinning, thus they are likely to be cheaper than membranes produced via electrospinning^[22]. The characterization of the technique and the nanofibers it produces will advance the accessibility of water filtration in areas of need, preventing disease and death due to contaminated drinking water supplies. A major focus point throughout this project will be to keep sunk-cost capital and operating costs low, and to create a procedure which is easily repeatable with consistent results.

Results and Discussion

In this report, we describe the design of a nanofibrous mat. We expect that best performance will be achieved by deposition of a 20 μm layer of PLA nanofibers, with a pore size of 0.2 μm supported by a porous scaffold with closely packed 0.225 mm radius holes. Upon completion of successful prototyping

using the blow spinning technique, we found fiber diameters of 200-400 nm using SEM and a Young's modulus and yield strength of 20.8 MPa and 850 kPa respectively using DMA.

Conclusions

The initial goal of this project was to investigate methods to create nanofiber membrane filters. After selecting solution blow spinning as our membrane production method, we then completed computational modeling of the fiber mats, mathematical modeling, initial prototyping and testing. For the filter design, the most notable relationship affecting the final filter performance is the relationship between the fiber diameter and the pore size of the filter. Fortunately, the fiber diameter is easily controllable through the solution blow spinning method by adjusting both the polymer solution concentration and flow rate. As fiber diameter decreases, pore size decreases, so it is important that our fiber diameter remain in the range of 100-300 nm in order to achieve the 0.2 μ m pore size necessary to filter out harmful pathogens.

We also discussed the important mathematical relationship between fiber mat thickness, burst pressure of the membrane, and flux through the filter. The fiber thickness and burst pressure are directly related; when the membrane is thicker, it is able to withstand more pressure. However, at the same time, the flux through the membrane will decrease due to the longer path length through the filter. These competing variables can be optimized for high flow through the filter, but we determined that for realistic flow rates, a supporting mechanism must be used. By using a porous scaffold with its own optimization parameters, we were able to design a thin, high flux membrane with commercially competitive permeabilities.

Finally, we were able to prototype and then characterize our mats using SEM and DMA to acquire morphology and material property data, which were used to further support our calculations. Proof of concept tests with vacuum filtration through our blow spun membranes produced promising initial results, though we do need to pursue further tests with quantitative data.

Future Work

Given more time, there are multiple avenues of research which could be pursued. To further our understanding of the nanofiber mat system, we hope to perform computational fluid dynamics (CFD) simulations using our generated fiber mats. This would allow us to analyze the effect of pressure differentials across our fiber membranes, and determine the velocity of the fluid through the pores. We would be able to determine tortuosity, and track particles as they progress through the fiber web.

Prototyping for this design project was limited to a small number of samples, only enough to capture the necessary data to enhance our model. We would also like to further characterize the morphology using a capillary flow porometer to determine pore size in detail. After filter characterization, the next step of the process would be to increase the number of samples, and perform flow testing in

order to see how well our produced mats compare to the theoretical models. This testing could include flow velocity testing, burst pressure, turbidity, and particulate filtration.

Because membrane fouling also plays a large role in filter lifespan, we would like to investigate the fouling properties of our filters and the most effective ways to prevent it from resulting in caking and clogging of the filter. Finally, in order to confirm that our filters would indeed be effective in a water purification system, we would utilize a sterile cell culture lab along with water filter testing and determine how well our filters can eliminate harmful pathogens from samples of water.

Acknowledgements

The University of Maryland

John Daristotle

Peter Kofinas

Robert Bonenberger

Raymond Phaneuf

Army Research Laboratories, Adelphi

Matthew Ervin

References

- [1] Mekonnen, M. M., & Hoekstra, A. Y. (2016). Four billion people facing severe water scarcity. *Science advances*, 2(2), e1500323.
- [2] Nasreen, S. A. A. N., Sundarrajan, S., Nizar, S. A. S., Balamurugan, R., & Ramakrishna, S. (2013). Advancement in electrospun nanofibrous membranes modification and their application in water treatment. *Membranes*, 3(4), 266-284.
- [3] "Membrane Disk Filters." Sterlitech, <http://www.sterlitech.com/filters/membrane-disc-filters.html> Web. 1 May 2016.
- [4] Medeiros, E. S., Glenn, G. M., Klamczynski, A. P., Orts, W. J., & Mattoso, L. H. (2009). Solution blow spinning: A new method to produce micro-and nanofibers from polymer solutions. *Journal of applied polymer science*, 113(4), 2322-2330.
- [5] Zhuang, X., Shi, L., Jia, K., Cheng, B., & Kang, W. (2013). Solution blown nanofibrous membrane for microfiltration. *Journal of Membrane Science*, 429, 66-70.
- [6] Li, Z., and C. Wang. "Effects of Working Parameters on Electrospinning." *One-Dimensional Nanostructures Electrospinning Technique and Unique Nanofibers*. N.p.: Springer, 2013. 15-28. Print.
- [7] Wang, R., Liu, Y., Li, B., Hsiao, B. S., & Chu, B. (2012). Electrospun nanofibrous membranes for high flux microfiltration. *Journal of Membrane Science*, 392, 167-174.
- [8] "Pore Size Chart." *Pore Sizes for Ultrafiltration, Microfiltration, Dialysis, and Macrofiltration at Spectrum Labs*. Web. 01 May 2016.
- [9] Leclerc, H., Schwartzbrod, L., & Dei-Cas, E. (2002). Microbial agents associated with waterborne diseases. *Critical reviews in microbiology*, 28(4), 371-409.
- [10] Baker, Richard W. "Overview of membrane science and technology." *Membrane Technology and Applications, Third Edition* (2012): 1-14.
- [11] Benko, Katie, Jorg Drewes, Pei Xu, and Tzahi Cath. "Use of Ceramic Membranes for Produced Water Treatment." *United States Department of the Interior Bureau of Reclamation* (2007): 21-57.
- [12] Wang, H. B., Mullins, M. E., Cregg, J. M., Hurtado, A., Oudega, M., Trombley, M. T., & Gilbert, R. J. (2008). Creation of highly aligned electrospun poly-L-lactic acid fibers for nerve regeneration applications. *Journal of neural engineering*, 6(1), 016001.
- [13] Sato, A., Wang, R., Ma, H., Hsiao, B. S., & Chu, B. (2011). Novel nanofibrous scaffolds for water filtration with bacteria and virus removal capability. *Journal of electron microscopy*, 60(3), 201-209.
- [14] Oliveira, Juliano E., Eduardo A. Moraes, José M. Marconcini, Luiz H. C. Mattoso, Gregory M. Glenn, and Eliton S. Medeiros. "Properties of Poly(lactic Acid) and Poly(ethylene Oxide) Solvent Polymer Mixtures and

- Nanofibers Made by Solution Blow Spinning." *Journal of Applied Polymer Science J. Appl. Polym. Sci.* 129.6 (2013): 3672-681. Web.
- [15] Li, Lin, Raed Hashaikeh, and Hassan A. Arafat. "Development of Eco-efficient Micro-porous Membranes via Electrospinning and Annealing of Poly (lactic Acid)." *Journal of Membrane Science* 436 (2013): 57-67. *Science Direct*. Web. 12 Apr. 2016.
- [16] Bui, N. N., Lind, M. L., Hoek, E. M., & McCutcheon, J. R. (2011). Electrospun nanofiber supported thin film composite membranes for engineered osmosis. *Journal of Membrane Science*, 385, 10-19.
- [17] "Water." Viscopedia. Retrieved March 23, 2016, from <http://www.viscopedia.com/viscosity-tables/substances/water/>
- [18] Chen, Pei, "A Preliminary Discourse on Adhesion of Nanofibers Derived from Electrospun Polymers" (2013). Department of Mechanical Engineering. Paper 675.
- [19] "Durapore Membrane Filters." EMD Millipore. Retrieved March 23, 2016, from http://www.emdmillipore.com/US/en/product/Durapore-Membrane-Filters,MM_NF-C7631
- [20] Rosato, D. V., & Rosato, M. G. (2012). *Injection molding handbook*. Springer Science & Business Media.
- [21] "The Best Known Packings of Equal Circles in a Square (up to N = 10000)." *Packomania*. Web. 08 May 2016.
- [22] Souza, Michelle Andrade, Karine Yamamura Sakamoto, and Luiz Henrique Capparelli Mattoso. "Release of the diclofenac sodium by nanofibers of poly (3-hydroxybutyrate-co-3-hydroxyvalerate) obtained from electrospinning and solution blow spinning." *Journal of Nanomaterials* 2014 (2014): 56.
- [23] W.K. Schomburg, Introduction to Microsystem Design, RWTHedition, DOI 10.1007/978-3-642-19489-4_6, # Springer-Verlag Berlin Heidelberg 2011